

## SIMULATION OF A TWO-PARALLEL-PLATE COLLECTOR

M.M. El-Kassaby

Mechanical Engineering Department  
Faculty of Engineering, Alexandria University  
Alexandria, Egypt

### Abstract

A computer program was used to simulate a solar heating system operated by thermosiphon action. The system consists of a two-parallel-flat-plate collector and a storage tank.

The computer model takes into consideration the natural heat convection between the two parallel plates, losses from the top and the bottom of the collector, energy balance for the collector, variation of solar incident insolation, variation of the collector tilt angle, losses from the storage tank, heat balance for the storage tank with and without withdrawing a load, and variations of the ambient temperature.

The experimental set up consists of a two-parallel-plate collector. The plates have an area of  $76 \times 76 \text{ cm}^2$  and spaced by 1 cm. The capacity of the storage tank is 42 liters, equipped with three thermocouples at three different locations to measure the tank temperature.

Comparison between simulation and experimental results shows a good agreement.

Nomenclature

- $A_c$  collector surface area,  $m^2$   
 $a$  distance between two plates, m.  
 $c_p$  specific heat at constant pressure,  $kJ/kg \text{ }^\circ K$   
 $c_{ps}$  specific heat for steel,  $kJ/kg \text{ }^\circ K$ .  
 $g$  gravity acceleration,  $m/s^2$   
 $Gr$  local Grashof number =  $\frac{g \beta (T - T_{b2}) x^3}{\nu^2}$   
 $h$  local heat transfer coefficient,  $w/m^2 \cdot ^\circ C$   
 $k$  thermal conductivity,  $w/m \cdot K$   
 $L$  length in x direction, m.       $Nu$  Nusselt number  $[hx/k]$   
 $N$  number of glass covers.       $Pr$  Prandtl number  $[\mu c_p/k]$   
 $t$  time, sec.       $t_1$  plate thickness, m.  
 $T$  temperature,  $^\circ C$        $u$  velocity, m/s  
 $U$  overall heat transfer coefficient,  $W m^{-2} K^{-1}$        $V$  wind speed, m/s.  
 $W$  the width of the two parallel plate, m.  
 $x$  direction along the length of the plate, m.  
 $y$  direction perpendicular to the plate, m.

Subscripts

- $a$  ambient       $b_1$  upper plate.       $b_2$  lower plate  
 $i$  insulation, also inner       $c$  outer       $s$  steel  
 $tank$  tank       $w$  water

Greek-Symbols

- $\beta$  The coefficient of volume expansion,  $1/K$   
 $\rho$  density,  $kg/m^3$        $\nu$  kinematic viscosity,  $m^2 s^{-1}$   
 $\theta$  collector tilt angle       $\psi$  stream function  
 $\sigma$  stefan-Boltzman constant =  $5.67 \times 10^{-8}$ ,  $W/m^2 k^4$   
 $\epsilon_{p,i}$  infrared emittance of the plate. (0.9)  
 $\epsilon_{g,i}$  infrared emittance of the cover. (0.9)

## 1. Introduction

This study presents detailed simulation for two-parallel-plate solar collectors. The collector simulation studies have a great importance for the following reasons:

1. Collector simulation necessitates and provides better understanding of the collector variables (such as tilt angle, dimensions, thickness of insulation, etc.) and their effects on system performance.
2. Collector simulation reduces the amount of the required collector testing.
3. Collector simulation provides a tool in optimizing a system design for a particular application.
4. Collector simulation can predict the system performance at different consumed loads.

Many investigators (see Ref. 1, Chapter 4) have introduced methods to calculate the collector efficiency for tube collector or collector with flow ducts of rectangular cross-section. None of them, (to the knowledge of the author) has reported a complete system simulation for two-parallel-plate collectors, which is the aim of the present work.

For further check on the proposed model, a complete experimental set-up was built and a comparison between the simulation results and experimental ones is given.

## 2. Theoretical Analysis

The problem of heat transfer by natural convection between two parallel plates has been solved by El-Kassaby [2]. The solution was in the form

of momentum and energy equations, which predict velocity and temperature distributions at any required cross section, as follows:

$$F''' + \varphi \sin \theta + [(n+3) FF'' - 2(n+1)F'] = 0 \quad (1)$$

where the first, second, and third terms represent viscous, buoyancy, and inertia forces, respectively.

$$\frac{\varphi''}{Pr} + [(n+3) \varphi' F - 4nF' \varphi] = 0 \quad (2)$$

where the first term represents heat conduction while the second is the heat convection term.

where  $F$  is a function of  $\eta$ , with

$$\eta = \frac{y}{x} \left[ \frac{g\beta(T - T_{b2}) x^3}{4\nu^2} \right]^{0.25} = \frac{y}{x} \left[ \frac{Gr(x)}{4} \right]^{0.25}$$

$$\psi = 4\nu \left[ \frac{Gr(x)}{4} \right]^{0.25} F(\eta), \quad (3)$$

where  $\psi$  is the stream function, and

$$\varphi = \frac{T - T_{b2}}{T_{b1} - T_{b2}}$$

The boundary condition for equations (1 and 2) are

$$\begin{aligned} \text{at } y = 0 : \eta = 0, \quad F(0) = 0, \quad \varphi = 1 \\ y = a : \eta = \eta_1, \quad F(\eta_1) = 0, \quad \varphi = 0 \end{aligned} \quad (4)$$

Since equations (1,2) are ordinary nonlinear differential equations, therefore, their exact solution is quite difficult. The solution has been performed using a finite difference explicit method with an axial interval of  $x = L/100$  and perpendicular interval of  $y = a/30$ .

Applying the finite difference methods to equations 1 and 2 with boundary conditions given in equation 4, 28 simultaneous equations for each  $F$  and  $\phi$  were obtained. More details are given in ref. [2].

### 2.1 Energy Balance for the Collector

The energy balance for the control volume of a segment in the  $x$  direction (see Fig. 1) is given as:

$$q_{in} + q_4 = q_1 + q_2 + q_3 + q_5 + q_6 + q_7 \quad (5)$$

where

$$q_{in} = I_c dA_c \Delta t = I_c \cdot \Delta x \cdot W \cdot \Delta t$$

= Total solar energy incident upon the plane of the collector (kJ).

$$q_1 = \Delta x \cdot W \cdot t_1 \cdot \rho_s \cdot C_{ps} (T'_{b1} - T_{b1})$$

= Internal energy increase in upper plate, (kJ).

$$q_2 = \Delta x \cdot a \cdot W (\rho' C'_p T'_{av} - C_p T_{av} \rho)$$

= Internal energy increase for the fluid inside the control volume, (kJ).

$$q_3 = \Delta x \cdot W \cdot t_1 \cdot \rho_s \cdot C_{ps} (T'_{b2} - T_{b2})$$

= Internal energy increase of the bottom plate, (kJ).

$$q_4 = u \cdot W \cdot a \cdot \rho \cdot T_{av} \Delta t$$

= Energy associated with the flow entering control volume, (kJ).

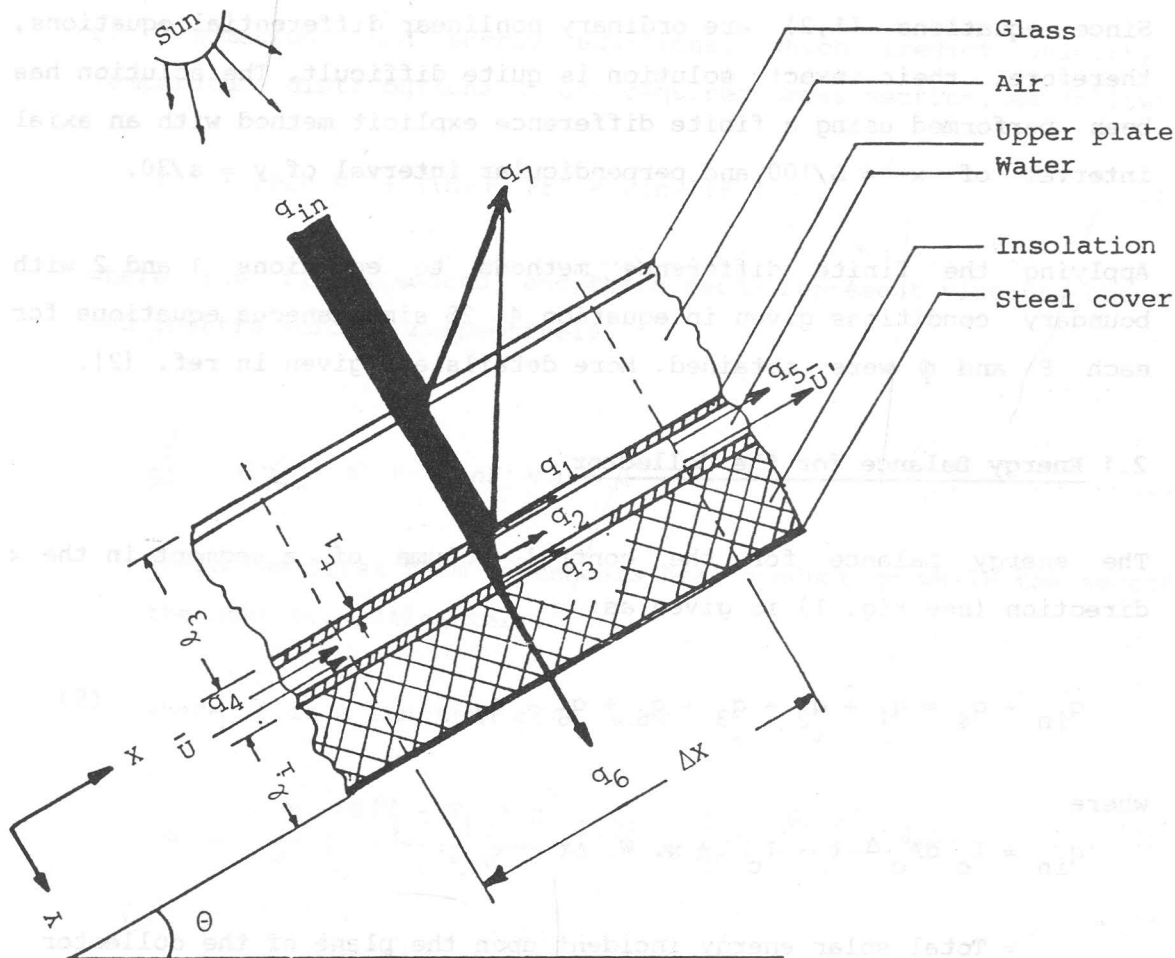


Fig. 1. Shows details of a segment of the two parallel-plates collector.

$$q_5 = u \cdot W \cdot a \cdot \rho T'_{av} \Delta t$$

=Energy associated with the flow leaving the control volume, (kJ)

$$q_6 = \text{The back losses (kJ).}$$

$$q_7 = \text{The top losses, (kJ).}$$

Notice that the (') implies the same variable as that calculated at the end of the period of time  $t$ .

For a collector of area  $\ell_1 \ell_2$  ( $\ell_1$  is in the x-direction), with an insulation height  $\ell_3$  from the sides, and with a layer of insulating material  $\ell_i$  thick at the bottom and along the side (Fig. 1), the effective back losses can be given as [3]:

$$q_{\text{back loss}} = \frac{A_c k_i}{\ell_i} (T_{b1} - T_a) \left[ 1 + \frac{(2\ell_3 + \ell_i)(\ell_1 + \ell_2)}{\ell_1 \ell_2} \right] \quad (6)$$

where  $A_c$  is the surface area of the collector. The back losses from a segment ( $q_G$ ) can be calculated from equation (6) as :

$$q_G = q_{\text{back loss}} \frac{\Delta x}{1000 \ell_1} \cdot \Delta t \quad (\text{kJ})$$

The top losses can be calculated using the equation suggested by [3 & 4], which can be given as

$$q_{\text{top loss}} = \frac{(T_{b1} - T_a) A_c}{N \left\{ (C/T_{b1}) \left[ (T_{b1} - T_a) / (N+f) \right]^{0.33} + 1/h_{c,\infty} \right\} + \frac{\sigma (T_{b1}^4 - T_a^4) A_c}{1 / [ \epsilon_{p,i} + 0.05N (1 + \epsilon_{p,i}) ] + (2N+f-1) / \epsilon_{p,i} - N}} \quad (7)$$

where

$$f = (1 - 0.04 h_{c,\infty} + 0.0005 h_{c,\infty}^2) (1 + 0.091N)$$

$$C = 365.9 (1 - 0.00882\theta + 0.00013\theta^2)$$

$$h_{c,\infty} = 5.7 + 3.8 v$$

The top losses from the segment  $q_7$  can be calculated as

$$q_7 = q_{\text{top loss}} \frac{\Delta x}{1000 \ell_1} \cdot \Delta t$$

## 2.2 Energy Balance for the Storage Tank

The energy balance of storage tank can be written as:

$$q_8 = q_9 + q_{10} + q_{11} + q_{12} + q_\ell \quad (8)$$

where

$q_8$  = energy associated with the flow entering the storage tank, coming from the collector (kJ).

=  $q_4$  for the last segment

$q_9$  = heat losses from the top and bottom of the collector, (kJ).

$$= U_1 \frac{\pi D^2}{2} (T_{\text{tank}} - T_a) \Delta t$$

$q_{10}$  = losses from the surface area of the storage tank, (kJ).

$$= U_2 \pi DL (T_{\text{tank}} - T_a) \Delta t$$

$q_{11}$  = energy associated with the flow leaving the storage tank and entering to the collector, (kJ).

$$= u W. a. c_{pw} \cdot T_{\text{tank}} \cdot \Delta t$$

$q_\ell$  = the energy associated with the load consumed by the user, (kJ)

$$= m c_{pw} (T_{\text{tank}} - T_{\text{fresh water}})$$

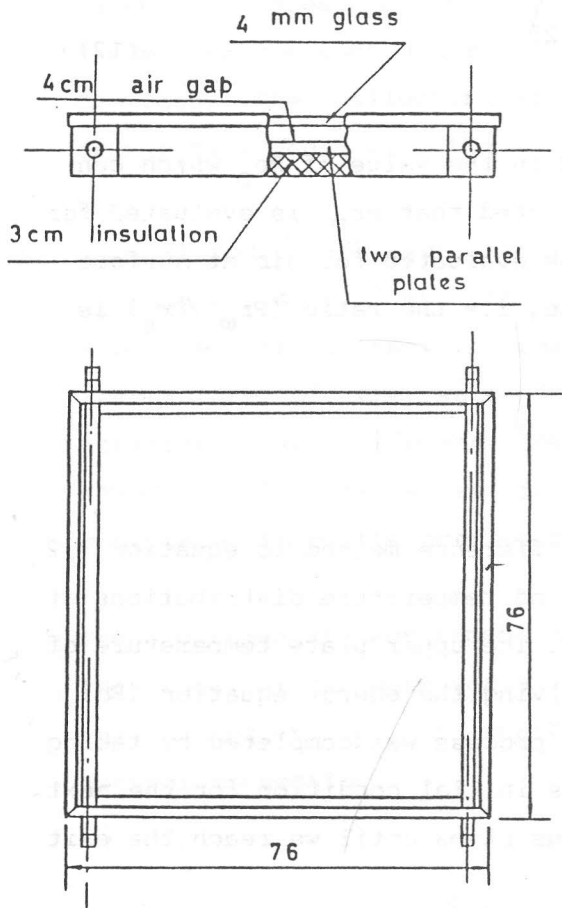
The overall heat transfer coefficient, for the top and bottom surfaces of the storage tank can be evaluated as:



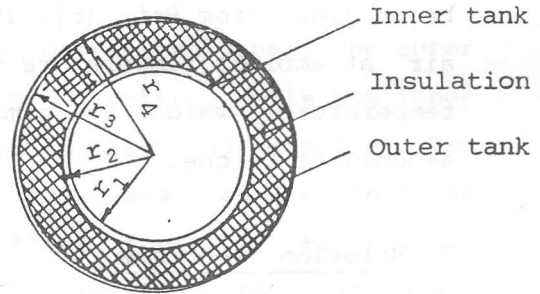
$$\frac{1}{U_1} = \frac{1}{h_j} + \frac{1}{h_c} + \frac{t_s}{k_s} + \frac{l_i}{k_i} \quad (9)$$

where,  $t_s$  is the thickness of the steel, used to fabricate the storage tank. The over all heat transfer coefficient for the cylindrical storage tank surface can be evaluated as [5] (see Fig. 2.b)

$$\frac{1}{U_2} = L \left( \frac{1}{r_1 h_i} + \frac{\ln(r_2/r_1)}{k_s} + \frac{\ln(r_3/r_2)}{k_i} + \frac{\ln(r_4/r_3)}{k_s} + \frac{1}{r_2 h_o} \right)$$



(a)



(b)

Fig. 2. a) Details of the two parallel plates collector; b) Cross section of the storage tank.

The inner heat transfer coefficient inside the storage tank can be evaluated as [5]

$$\text{Nu}_D = \frac{h_i D_i}{k_w} = 3.66 \quad (11)$$

In the previous equation, it is assumed that the flow inside the tank is a fully developed laminar flow.

Zhukauskas [6], has performed the most comprehensive study of flow normal to single tubes and gave the following empirical formula:

$$\text{Nu}_D = \frac{h_c D_o}{k_{\text{air}}} = C \text{Re}^n \text{Pr}^{0.37} \left( \frac{\text{Pr}_\infty}{\text{Pr}_s} \right)^{0.25} \quad (12)$$

Where  $C$  and  $n$  are constants that depend on the value of  $\text{Re}_D$  which can be obtained from Ref. [6]. It is to be noted that  $\text{Pr}_\infty$  is evaluated for air at ambient temperature while  $\text{Pr}_s$  is evaluated for air at surface temperature, which is almost the same, i.e the ratio  $(\text{Pr}_\infty / \text{Pr}_s)$  is assumed to be one.

### 3. Solution Technique

For each segment, applying the finite difference method to equation 1,2 as explained in ref. [2], the velocity and temperature distributions at the end of the segment can be obtained. The upper plate temperature of segment  $j$   $T_{b_1}(j)$  can be obtained by applying the energy equation (Eq. 5) and using an iteration method. The process was completed by taking the final condition from station  $j$  as initial condition for the next segment  $(j+1)$  and repeating the previous steps until we reach the exit cross section from the collector.

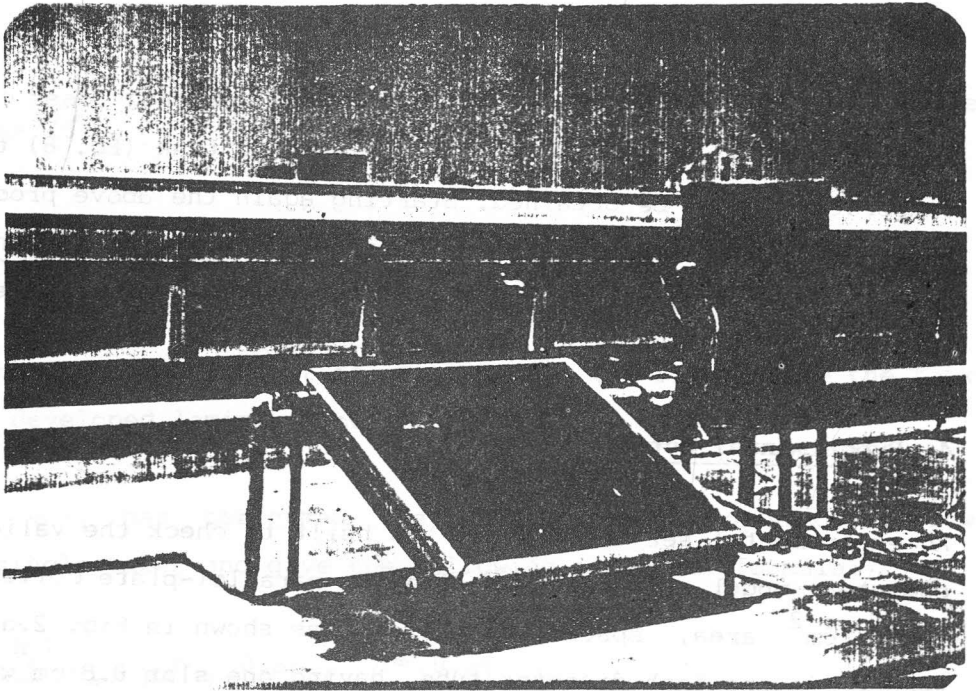
Applying the energy balance to the storage tank (Eq. 8) the new tank temperature can be obtained. Starting again the above procedure using this new tank temperature as initial condition for the next time interval, and repeating the whole procedure till any required period of time.

#### 4. Experimental Set-Up

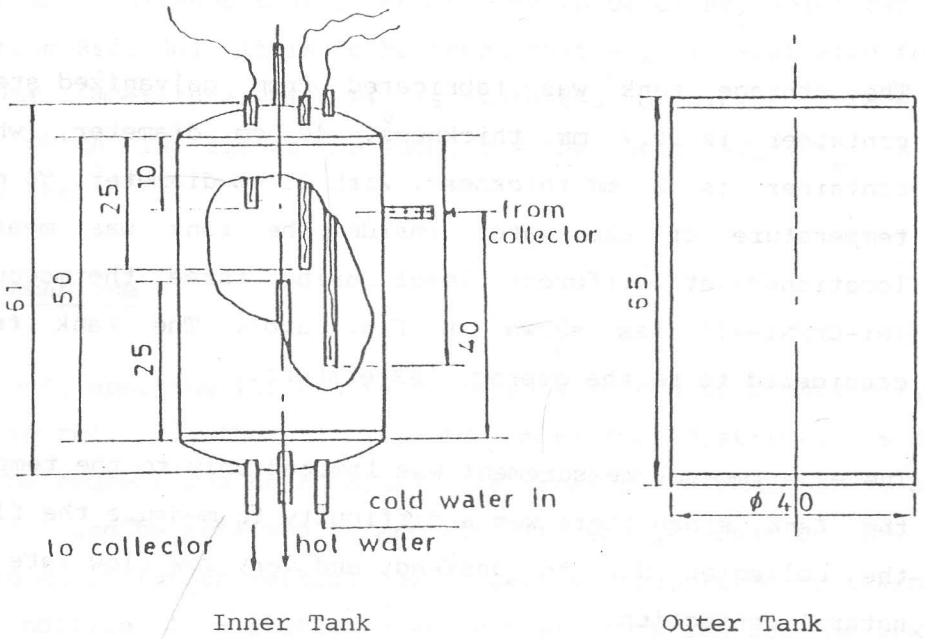
An experimental set-up (Fig. 3) was built to check the validity of the computer model. It consists of a two-parallel-plate collector having  $76 \times 76 \text{ cm}^2$  area, spaced by 1 cm (as shown in Fig. 2.a) and its feeder is one inch diameter tube, having one slot 0.8 cm wide, and 65 cm long. The collector has been selected to face the south with 25 degree tilt angle with the horizontal surface.

The storage tank was fabricated from galvanized steel. The outer container is 0.7 mm thickness, 40 cm diameter, while the inner container is 2 mm thickness, with 33 cm diameter, 50 cm height. The temperature of the water inside the tank was measured in three locations at different level using three thermocouples type K (Ni-Cr/Ni-Al) (as shown in Fig. 3.b). The tank temperature was considered to be the average temperature.

The experimental measurement was limited only to the temperature inside the tank, since there was a difficulty to measure the flow rate inside the collector due to unsteady and very low flow rate resulting from natural convection.



(a)



(b)

Fig. 3. a) Shows the two parallel-plates collector (fabricated and operated at Mu'tah University, Jordan)  
 b) Details of the storage tank. (Dimension in cm)

## 5. Results and Discussion

Typical results of the simulation model are tabulated in table 1 and plotted in figures 4,5 and 6. The experimental results taken on September 8, 1988 at Mu'tah University, Jordan, Starting time at 9:36 AM, are tabulated in table 2 and plotted in Fig. 4 for comparison with simulation results for the raise of the storage tank temperature.

Table 1. Samples of the simulation results

Time	T <sub>Tank</sub> °C	$\eta_c$	$\eta_s$	Qx10 <sup>-4</sup> m <sup>3</sup> /s	u cm/s	T <sub>av</sub> °C	I <sub>c</sub> kw/m <sup>2</sup> Meas.	T <sub>in</sub> -T <sub>ax</sub> x100 I <sub>c</sub>
00	36.2	0.00	0.00	0.000	0.000	00.00	0.00	0.000
10	36.2	7.32	4.88	0.153	0.011	36.70	0.67	1.705
20	36.6	34.30	31.92	0.655	0.043	41.74	0.74	2.085
30	37.5	67.19	64.80	0.960	0.063	44.54	0.78	2.315
40	38.8	84.16	81.59	1.143	0.075	46.30	0.80	2.457
50	40.2	84.80	82.06	1.222	0.080	47.40	0.82	2.514
60	41.6	80.40	77.44	1.270	0.083	48.30	0.84	2.532
70	42.9	77.16	74.02	1.331	0.087	49.27	0.87	2.555
80	44.2	75.60	72.30	1.399	0.092	50.28	0.89	2.605
90	45.5	74.20	70.78	1.470	0.097	51.32	0.91	2.658
100	46.9	73.57	69.89	1.550	0.102	52.40	0.93	2.707
110	48.3	72.83	68.98	1.625	0.107	53.51	0.95	2.760
120	49.6	72.25	68.22	1.792	0.113	54.60	0.97	2.820
130	51.0	71.45	67.22	1.805	0.119	55.70	0.98	2.904
140	52.4	70.00	65.60	1.878	0.125	57.30	0.98	2.997
150	53.7	68.24	63.56	1.942	0.130	58.30	0.98	3.098
160	54.9	67.47	62.68	2.010	0.134	58.90	0.98	3.137
170	56.2	66.90	61.94	2.080	0.137	60.01	0.98	3.197
180	57.5	66.57	61.58	2.204	0.145	61.10	0.99	3.228
190	58.7	65.12	59.86	2.234	0.147	62.19	0.99	3.335
200	59.9	62.86	57.40	2.280	0.150	63.18	0.98	3.450

Table 2. Experimental results (Sept. 8, 1988).

Time minute	00	20	39	59	75	92	129	144	188
Tav °C	36.2	36.9	37.5	41.6	44.1	47.0	50.3	47.9	52.1

Figure 4 shows the tank temperature variation versus the time. It is clear from the figure that the simulation model gives good agreement with the experimental results up to time 130 minutes, after which it deviates clearly. This could be due to weather fluctuation in wind

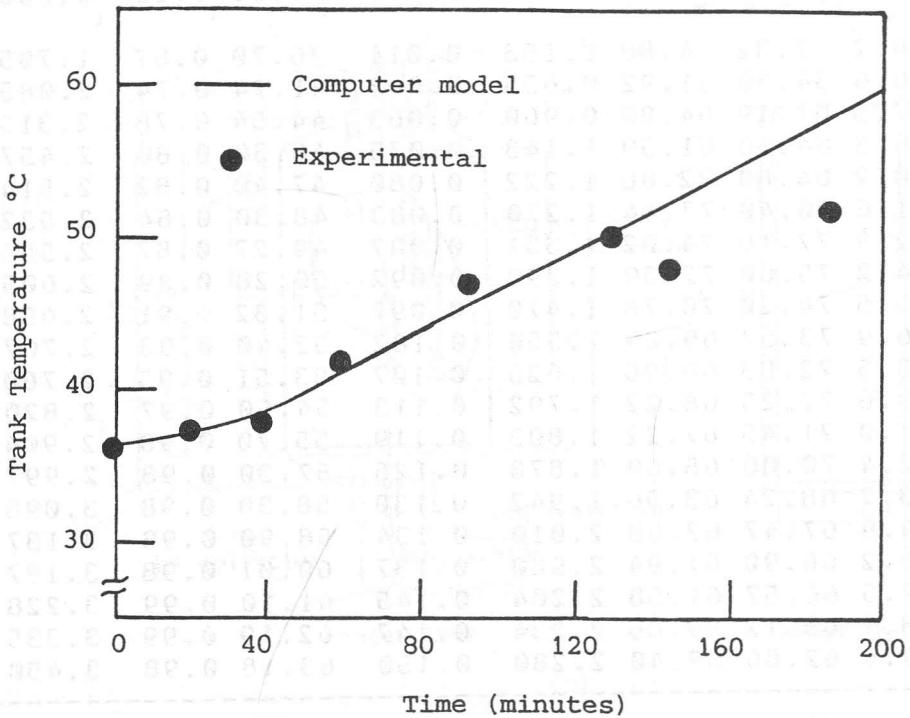


Fig. 4. Shows the storage tank temperature variation versus the time.

in spite of having a clear sky.

Figure 5 shows the variation of system and collectors efficiencies as a function of time. The collector efficiency was calculated as

$$\eta_c = \frac{u_a W \Delta t (T_{av} - T_{in})}{I_c A_c \Delta t} \quad (13)$$

the system efficiency was calculated as

$$\eta_s = \frac{V_{Tank} \rho_w \Delta T_{tank}}{I_c A_c \Delta t} \quad (14)$$

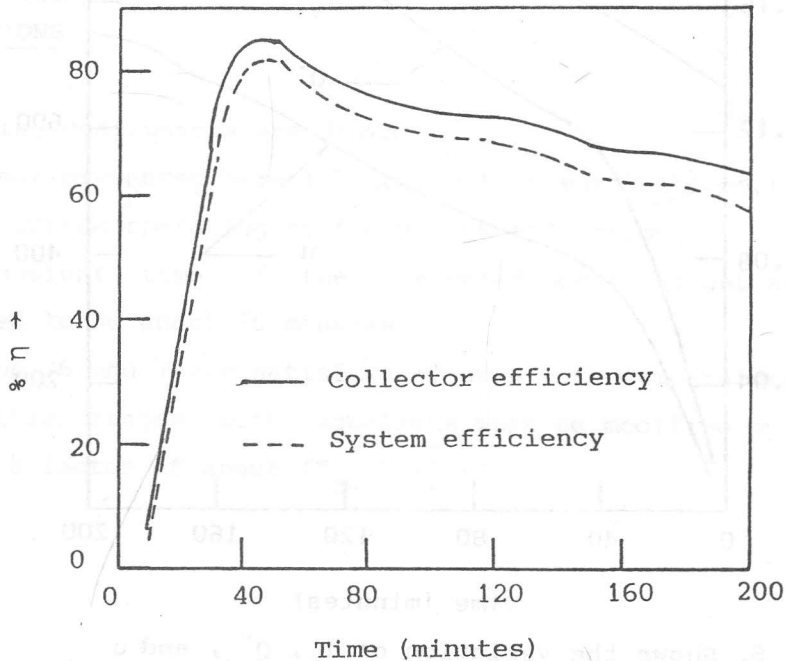


Fig. 5. Shows the system and collector efficiencies.

Both efficiencies are increasing initially for a certain time up to a maximum value, then start to decrease. This is due to a transient effect as during the starting period of calculation the model is adjusting itself to build up a certain temperature distribution along the collector plates. It looks like that initially the major part of received energy is consumed as internal energy for both collector plates and the water inside the collector. This time is predicted to be 50 minutes. After this transient period the efficiency decreases as the temperature increases due to the increase in losses.

Figure 6 shows the variation of the calculated values of volume

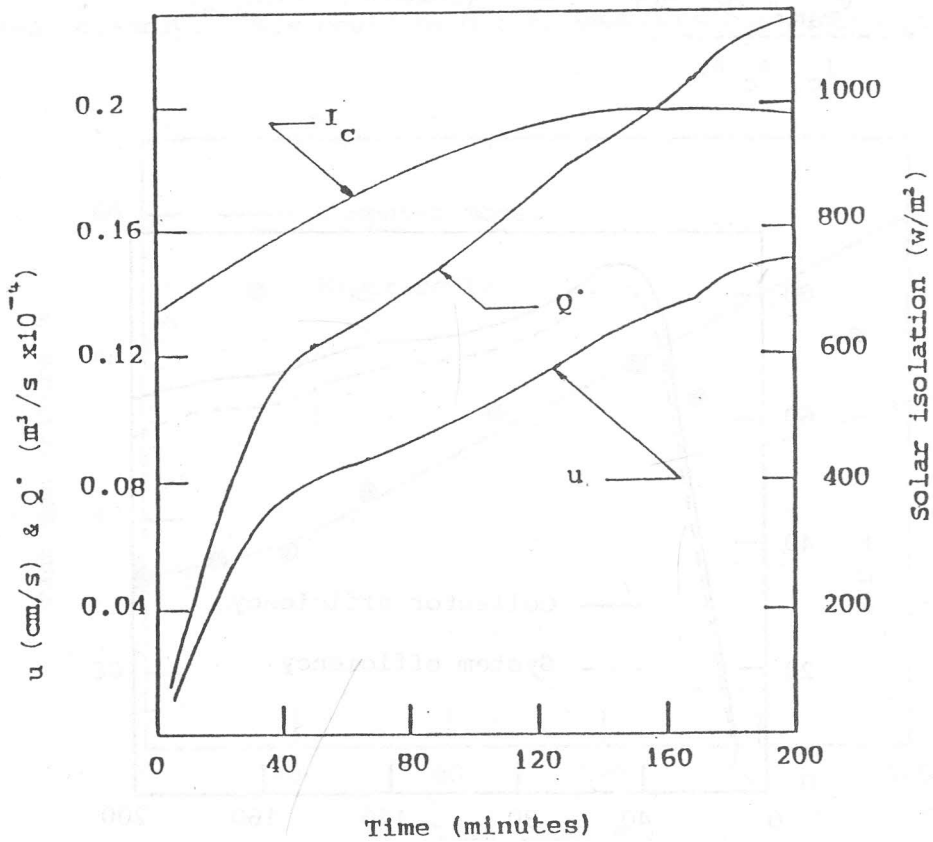


Fig. 6. Shows the variation of  $I_c$ ,  $Q^{\cdot}$ , and  $u$  versus the time.



discharge ( $Q$ ), average velocity out of the collector ( $u$ ), and the measured solar isolation. If one considers the transient time as 50 minutes, it can be noticed that as the temperature increases, both  $Q$  and  $u$  increase almost linearly. This is due to the fact that as the temperature increases on the upper plate, more driving force (density difference) will be created, resulting in an increase in average velocity and consequently an increase in  $Q$ .

It is noticed from the simulation results that, the tank temperature increases rapidly after it passes the  $50^{\circ}\text{C}$  range. The author believes that this is due to the underestimation heat of the losses in the empirical formula (6 and 7). This was overcome by using an empirical adjusting factor of  $(T_{av}/50)^3$ .

## 6. CONCLUSIONS

The following conclusions are drawn:

1. The model presented here is capable to predict the performance of a heating system operating by thermosiphonic action.
2. The transient time of the presented model (to get stability) is predicted to be about 50 minutes.
3. Equations 6 and 7 are satisfactory up a tank temperature of  $50^{\circ}\text{C}$ . Above this ranges both equations must be modified by multiplying them by a factor of about  $(T_{av}/50)^3$ .

**References**

- [1] Kreith, F. J. F. Kreider, Principles of Solar Engineering, McGraw Hill, 1978.
- [2] El-kassaby M. M., A Numerical Approach for Solution of Convection Heat Transfer Problem Between Two Parallel Plates, Alex. Eng. J., Alex. Univ., Vol. 27, No. 2, PP. 37-54 (1988).
- [3] Hottel, H.C., and B.B. Woertz, Performance of Flat-Plate Solar-Heat Collectors, Trans. ASME, Vol. 64, P. 91, 1942.
- [4] Klein, S., A., Calculation of Flat-plate Collector loss Coefficient, Sol. Energy, Vol. 17, PP. 79-80, 1985.
- [5] Chapman, J. Alan, Heat Transfer, Fourth edition, Collier Macmillan, 1984.
- [6] Zhukauskas, A., Heat Transfer from Tubes in Crossflow, Advances in Heat Transfer, Vol. 8, New York, Academic Press, 1972, P. 93.